Challenges and Approaches - Probing Tumor Cell Invasion by Atomic Force Microscopy

Thomas Ludwig* [1], Robert Kirmse[1], Kate Poole[2]

[1] German Cancer Research Center, Group Microenvironment of Tumor Cell Invasion, Postal Address: BIOQUANT Center, BQ0009 NWG Ludwig, Im Neuenheimer Feld 267, 69120 Heidelberg, Germany

[2] JPK Instruments AG, Bouchestrasse 12, 12435 Berlin, Germany

Metastasis is a complex and highly dynamic process that depends essentially on the ability of cancer cells to invade and actively remodel intact tissue structures. Pericellular proteolytic activity is a prerequisite for tumor cells to achieve this aim and constitutes a final common pathway of all invasive malignancies. The extracellular matrix exerts an ambivalent function upon tumor cell invasion: physical obstacle and structural support. Cancer cells have to balance these entities and coordinate proteolysis in time and space for the effective remodelling of their microenvironment. Little is known about the distinct regulatory mechanisms which are involved in this process. The system's critical determinants - proteolytic activity and biophysical parameters - are well accessible by Atomic Force Microscopy (AFM), a unique tool for functional, nanoscale probing and morphometric, high resolution imaging of processes in live cells. This review highlights basic mechanisms of tumor cell invasion and focuses on application examples of AFM techniques for their investigation.

Keywords: Atomic Force Microscopy; cancer; invasion; metastasis; microenvironment; protease; morphometry; force spectroscopy; force mapping; adhesion, confocal microscopy

1. Introduction

Invasion of adjacent tissues is a defining feature of malignancy in tumors. Subsequent metastasis, characterized by the spread of cancer cells to sites distant from their origin, accounts for more than 90 % of all lethal outcomes in cancer [1]. Patients can be healed by local treatment of the tumor, for example complete excision, until it has broken its boundaries. The chances for successful treatment are limited once this threshold has been crossed. Accordingly, the early detection of small tumors remains the most promising method to improve the life expectancy of affected patients [2]. This forms the rationale for extensive screening programs for treatable common tumors [3]. Despite this, up to two thirds of patients have metastasis when being initially diagnosed with cancer [4]. Unfortunately, metastasis is frequently the first occasion when cancers become clinically apparent and have already started to compromise the function of an organ due to compression or erosion of vital structures.

The formation of metastasis is the result of a coordinated, multistep series of events (table 1). However diverse, all solid neoplasms have to acquire the same abilities in order to metastasize. These properties include both, gain and loss of specific functions compared to the cells from which a certain type of cancer descends. Cancer cells lose the sensitivity to anti-growth signals, but gain limitless replicative potential, self sufficiency in growth-signals and the ability to invade and remodel intact tissue structures and display abnormal adhesion to extracellular matrix (ECM) and neighbouring cells [1, 5]. Morphological alterations on the single cell level and perturbation of normal tissue organization reflect this altered functionality and constitute the basis for the histological diagnosis of cancer.

*Corresponding author; e-mail: t.ludwig@dkfz.de; phone: +49(0)6221-5451234

The local host tissue is a constant participant during tumor development and metastasis [6]. For example, the expansion of tumors is limited by nutritient and oxygen supply. Angiogenesis, the sprouting of new vessels, alleviates this restriction and facilitates dissemination of cancer cells by granting them access to the bloodstream. Nonetheless, metastasis is less the result of passive carriage of tumor cells by the blood- or lymph stream than an active, regulated process.

Table 1 Milestones of the metastatic cascade [3, 7]

- cell detachment from the primary tumor mass
- invasion of surrounding tissue structures
  - remodelling of the microenvironment
  - angiogenesis
  - cancer cell migration
  - degradation of physiological barriers
- penetration of the vascular lumen (intravasation)
- distribution
  - survival in the circulation
- adhesion to distant endothelia
- penetration of the vascular lumen (extravasation)
- proliferation in a new environment.

The cleavage of basement membrane proteins by proteases is an early event of the metastatic cascade [8, 9]. Proteases are crucial for most of the common capabilities cancers acquire during their development [10, 11]. Their function constitutes a final common pathway of all invasive neoplasms. Regulated proteolytic activity is a prerequisite for tumor cells to balance i) attachment to and detachment from the ECM, ii) the ECM's biomechanical properties, and iii) the overall structure of their microenvironment. (Fig. 1). Despite being a physical obstacle, the ECM still has to provide sufficient resistance to allow the cancer cells to develop traction for migration. In order to remodel the microenvironment in such a defined manner, the function of proteolytic activity in tumor cell invasion has to go beyond a simple "path clearing process" [12]. Furthermore, proteolytic cleavage during tumor cell invasion is not restricted to ECM components. Chemokines, their receptors, adhesion molecules, clotting factors and proteinase inhibitors and proteases have been identified as important targets of tumor cell associated proteases [10, 13-16].

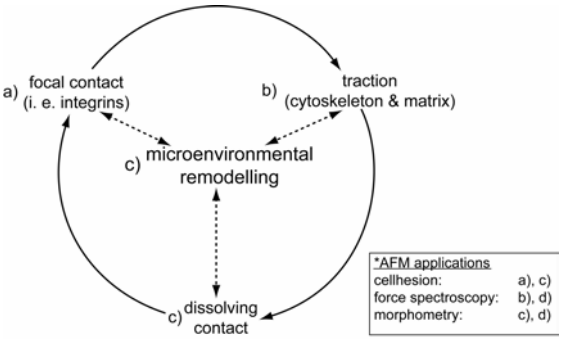

Fig. 1 Tumor cell migration and invasion.
a) Cancer cells establish focal adhesions to the extracellular matrix. **b)** The cancer cell's cytoskeleton generates force which is transmitted via these focal adhesions and results in traction for effective locomotion. **c)** Adhesions are dissolved by localized, proteolytic activity. **d)** Proteolytic activity is critical for the remodelling of a cancer cell's microenvironment i.e. the generation of physical defects in the ECM.

The functionally relevant proteolytic net activity in a cell's microenvironment results from the fragile, local balance of miscellaneous proteases, their substrates, and inhibitors [7]. The interplay of proteolytic activity and biomechanics make a continuous adjustment and optimization of these parameters

necessary (Fig. 1). Hence, cancer cells have to have effective mechanisms to sense force, geometry and mechanotransduction in relation to their microenvironment. Basic principles of this process and the integration of feedback signals into the spatiotemporal regulation of proteolytic activity remain to be elucidated.

In principle, by employing different AFM techniques, the kinetics of the system's determinants described above can be addressed. This renders AFM an unique tool for the direct investigation of basic mechanisms in metastasis and tumor cell invasion. The application examples presented here – morphometric imaging, force spectroscopy and single cell force spectroscopy using the CellHesion module – cover essential aspects of this process.

2. Morphometic Imaging of Pericellular Proteolytic Activity

2.1 Biological Background and Rationale

Proteases are potent regulators of cellular microecology and drive fundamental physiological and pathological processes, ranging from embryogenesis to inflammation [10]. There is virtually no biological process involving tissue remodelling which does not rely on it [17]. Activated endothelial cells utilize for example pericellular proteolytic activity for ECM remodelling and neovascularization displays in general striking similarity to tumor cell invasion. [18, 19].

Given the impact of proteolytic activity on biological systems, precise quantification is essential to unravel its diverse effects. Still, its precise quantification faces two major challenges: excessive, posttranslational regulation and spatial restriction.

As subtle changes of proteolytic activity produce profound biological alterations, it has to be tightly regulated. Diverse mechanisms modulate net proteolytic activity. The activity of proteases is regulated at the transcriptional, translational and posttranslational level. Mechanisms of posttranslational regulation are comprised of the secretion, activation, inactivation, glycosylation, oligomerzation and trafficking of proteases and the expression of endogenous protease inhibitors. [3]. As a result of this extensive posttranslational regulation, the activity of a single protease cannot be extrapolated from its concentration. It must be considered, that in a cell's microenvironment containing variable, highly heterogeneous assortments of proteases, inhibitors and substrates may be present at different subcellular spots. The coherencies of this intricate network are just beginning to emerge, as the number of protease targets is constantly growing [20, 21]

In addition, proteolytic activity in cancer cell invasion is a very local phenomenon. Although a protease can be widely expressed throughout a tumor, it may for example only be active at the leading edge of a small subset of cells at the tumor-stroma interface. Several specific mechanisms that confine and concentrate protease activity in the pericellular microenvironment and cellular subdomains of tumor cells have been identified. These have been found to be essential for the invasion promoting activity of proteases (reviewed in [3])

The spatial restriction and the discrepancy of protease concentration and activity challenge the maximum achievable resolution of common imaging techniques and *in vitro* diagnostics. AFM overcomes these limitations and can be applied in the direct, functional quantification of pericellular proteolytic activity in cancer cells *in vitro*.

2.2 Atomic Force Microscopy and Morphometric Imaging

AFM evolved from the Nobel prize winning scanning tunnelling microscope (STM) [22]. The STM itself was the first instrument to generate real-space images of surfaces with atomic resolution. Several features distinguish AFM from other high resolution imaging techniques such as electron microscopy. AFM can process native biological samples under physiological conditions. This means foremost at

37°C in buffered media. The AFM is furthermore a mechano-optical device which acquires morphometric data. Morphometric implies that each data point has a defined x-, y-, and z-coordinate in space. By this means, topographic images with contrast based on structure are built. Colouration of topographic images are virtual, since any colour in the spectrum can subsequently be assigned to a specific height (z-dimension).

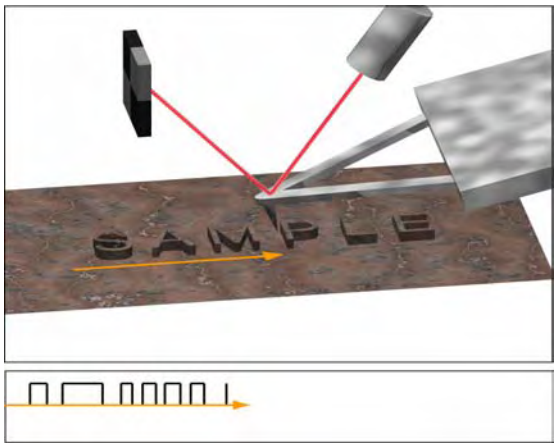

Fig. 2: Setup example for contact mode AFM. AFM utilizes the deflection of a thin silicon nitride spring with a fine probe at its end to reconstruct a 3D topographical map of sample surfaces A laser beam is focused at the end of the triangular spring (cantilever). Deflection of the spring is registered by a photo detector (left side). A feedback loop couples the photo detector to a piezo element at the other end of the silicon spring (not shown). The corresponding height is calculated from the physical constants of the piezo crystal and the voltage that must be applied to it in order to bring the laser beam back into the center of the photo detector. The AFM-tip is moved line wise (arrow) across the sample to collect x, y and z data.

The essential part of each AFM is an imaging stylus, composed of a soft cantilever with a sharp tip at its end. This stylus is moved line wise across the surface using piezo-electric elements (x-, and y-direction). A laser, focused at the cantilever, is reflected off the back of the cantilever onto a split photodiode. In general, two different modes of operation can be distinguished. The first mode is usually called static mode, as it records the static deflection of the cantilever. Any movement of the cantilever's tip caused by weak repulsive or attractive forces between the sample surface and the tip, results in the deflection of the laser. To maintain a constant force during scanning, the cantilever is moved vertically (z-direction) by another piezo-electric element in response to the features of the sample. The second mode is commonly referred to as the resonance mode, since the cantilever is oscillated at its resonance frequency via a feedback loop. Each mode offers a number of variations, each optimal for a distinct spectrum of applications. Operation in resonance mode enables for example non-contact, intermittent contact, phase imaging and force modulation mode scanning.

The maximum possible resolution of AFM is mainly determined by the shape of the tip at the end of the cantilever and sample properties. On purified proteins, reconstituted into a two dimensional lattice sub-nanometer scale features can be resolved. Features of approximately 20 nm can be identified on much more compliant living cells.

2.3 Quantification of Pericellular Proteolytic Activity

AFM can detect significant differences in average height, volume and molecular weight distribution of pericellular matrix proteins between the microenvironment of invasive cancer cells, distant control areas and the microenvironment of non-invasive cells [3, 23]. By treating it as the segment of a sphere, the molecular weight of a protein imaged by AFM can be calculated from the molecular volume of the structure [24]. In these experiments, the AFM registered significant changes in average matrix volume as little as 0.003 fl/μm^2 and decreases in average height of less than 0.5 nm. These studies revealed that the levels of proteolytic net activity in the microenvironment of cancer cells exceed the activity levels at a distance of 10 µm from these cells by several magnitudes, up to 10.000-fold in pancreatic carcinoma cells.

In summary, the AFM is capable of morphometric imaging and quantification of nanoscale ECM alterations in the cellular microenvironment. Considering that direct measurement of local proteolytic activity and high resolution imaging of ECM remodelling have proven difficult, this method is particularly advantageous as it enables functional evaluation on the subcellular level.

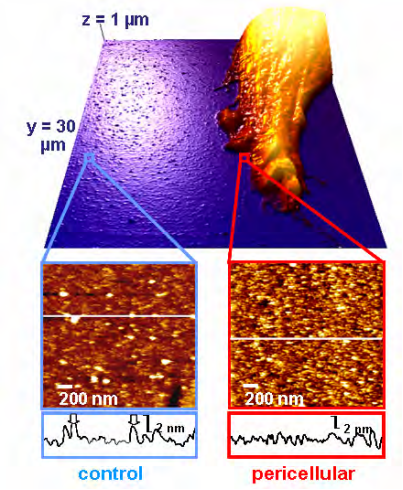

Fig. 3: Pericellular proteolytic activity. Melanoma Cells were seeded on a gelatine coated surface and imaged by AFM in contact mode. By decreasing the scanned matrix area (see magnified areas) structural features of the substrate coating become apparent. Matrix areas in the pericellular microenvironment display an increase in particle number and a decrease in particle size - the morphological correlate of proteolytic protein cleavage. As the AFM acquires primarily morphometric data when used for imaging, the average volume and height of such scanned areas above a given threshold, (defined by the lowest point in the coating) can be directly derived. As diameter and height of single proteins can be measured, their molecular volume can be calculated and their approximate molecular weight can be estimated.

3. Force Spectroscopy

3.1 Biological Background and Rationale

Cell-cell and cell matrix adhesions are vital for the organization of cells into tissues and are a prerequisite for the existence of complex organisms. Adhesion of cells is mediated by various integral membrane proteins, collectively termed cell-adhesion molecules (CAMs). Integrins represent the principal class of CAMs which is responsible for cell-matrix adhesion. However, even under physiological conditions detachment of cells and locomotion of normally non-motile cells may become necessary. Since adhesion factors “glue” cells to their surroundings and therefore impede cell migration, de-adhesion factors elicit the opposite effect. Disintegrins constitute for example one such class of de-adhesion factors. These small peptides contain the integrin binding RGD sequence, which is present in many ECM proteins. Binding of disintegrins to integrins thus blocks integrin-ECM interactions.

Proteases constitute another class of detachment regulating factors. Several direct and indirect effects of proteolytic activity on tumor cell adhesion and migration can be observed. The ability of cells to migrate on Laminin-5 is positively correlated with the expression of plasma membrane bound MT1-MMP (Membrane-Type 1 Matrix-MetalloProteinase) [25]. The same protease confers to transfected 3T3 fibroblasts the ability to migrate on myelin substrates [26]. Contrarily, a synthetic MMP-inhibitor and the tissue inhibitor of metalloproteinases-1 and -2, inhibit the migration of adenocarcinoma cells on gelatine matrix coated coverslips [27]. Silencing of MMP-9 in a Ewing’s sarcoma cell line, constitutively expressing MMP-9, resulted in a migratory-adhesive switch, marked by decreased spreading on ECM coatings and inhibition of migration towards fibronectin [28].

3.2 Force Spectroscopy

Given the mechanical nature of AFM, it be used for more than imaging purposes. The AFM is also a powerful tool for sensitive force measurements. Force spectroscopy, a dynamic analytical technique to study the mechanical properties of organic and inorganic samples at a nanoscale, is one such rapidly evolving AFM application. In principle, the AFM can quantify forces in the range of a single antibody-antigen interaction even in highly complex and heterogeneous biological samples. Instead of scanning line wise across the sample, the cantilever can be moved in a controlled fashion only in the z direction.

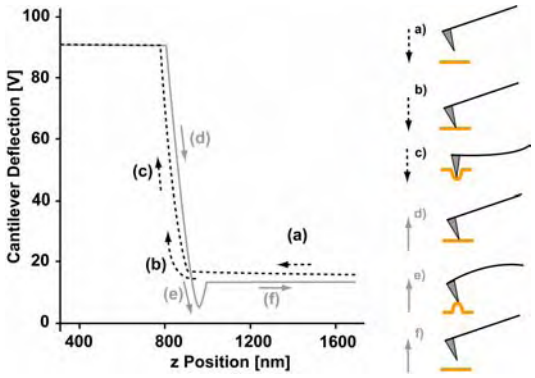

Fig. 4: AFM force plot. a) For a force curve, the deflection of the cantilever is measured as the AFM-tip approaches (a to c) and retracts (e to f) from the surface of a sample. Typically, the deflection is plotted against the vertical position of the piezo (z-position). **a)** The cantilever starts from a point where it is not in contact with the surface. **b)** After the tip made contact, **c)** the sample can be loaded with a controlled force by further approach of the tip, causing indentation of the sample. **d)** The cantilever is retracted and **e)** adhesion of the tip due to interaction with the sample can cause bending of the cantilever until **f)** the applied force is sufficient to separate the tip from the surface ("snap off point").

There are two key aspects to be considered, mechanically related to the vertical up- or down-movement of the cantilever:

i) The z piezo moves the cantilever directly towards the surface, until the cantilever begins to deflect. The deflection of the cantilever depends on the elastic properties of the cantilever and the surface. On a stiff sample, the deflection of the cantilever is directly proportional to the travel of the piezo. On soft samples, force application via the AFM-tip will result in an indentation [29]. This approach offers two alternative modes of measurement. Either the force which is necessary to yield a given extent of sample indentation (i.e. 200 nm), or inversely the indentation resulting from a given loading force (i.e. 100 pN) can be quantified. At the simplest level, the form of cantilever deflection curve is a qualitative measure for sample elasticity: the more compliant the surface the shallower the slope of the cantilever deflection (Fig. 3). According to Hooke's law, the loading force can be calculated from the deflection measured by the laser detection system and the spring constant of the cantilever. The cantilever's spring constant can be precisely determined by a variety of methods i.e. the thermal noise method. Indentation can be determined as the difference between the travel of the piezo and the deflection of the cantilever.

ii) The cantilever is retracted after it made contact with the surface. Any bonds between the cantilever and the surface will bend the cantilever towards the surface. As the bonds break, the cantilever will snap up and the specific force required to break the bonds can be calculated. There are many permutations of this type of experiment, from unfolding individual proteins, measuring protein-protein unbinding to cell-cell unbinding [30-34].

The firstly described approach can be used to probe samples biomechanically at specific regions [35].A combination of both, the approach and withdrawal information, can be utilized to investigate cell-cell or cell matrix interactions. Single cells can be attached to the cantilever and used for functional interaction probing of proteins (i.e. fibronectin coated surfaces), or other cells (i.e. endothelia) (Figs. 5 and 6).

3.3 The "Nano-Forklift" - Quantification of Single Cell Adhesion Forces

The information gleaned from force-spectroscopy experiments of cantilever-bound cells includes data on cell deformability, maximal unbinding forces, individual unbinding events and the total work required to remove a cell from the surface. However, this approach is challenging since it requires an increased vertical range of the AFM.

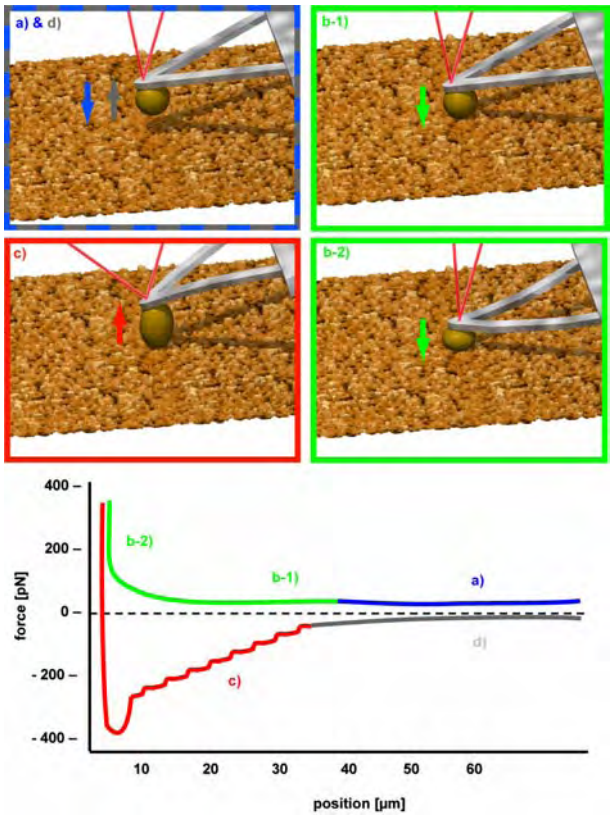

Fig. 5: Quantitative Force Spectroscopy of single Cells. The position given by the piezo element (x-axis) is plotted against the deflection of the cantilever (y-axis, representative of the applied force). There are two curves, one corresponding to the approach phase, where the cantilever-bound cell and the surface come into contact, the other is the retract curve where the cantilever-bound cell and the surface are pulled away from each other. In the initial phase of the approach curve (a) there is no deflection of the cantilever. After contact (b-1) the cantilever deflects, with the slope of deflection being determined, in part, by the elasticity of the cantilever-bound cell. When the desired deflection or force (the set point) is reached (b-2) the movement of the piezo element stops for a given contact time. As the cantilever-bound cell is separated from the surface any bonds between the cell and the surface will pull the cantilever towards the surface. As these bonds start to break the cantilever will snap up, corresponding to "jumps" in the force-distance curve (c). The size of these jumps indicates the force required to break the given interaction. After all of the bonds between the cell and the surface are broken, the cantilever will no longer be deflected and the piezo element will continue moving until a set separation distance is reached (d).

The control of contact and pulling conditions are critical for the study of cell adhesion using the force-spectroscopy mode of an AFM. Cells attach to surfaces via discrete entities. As the cell is pulled away from the surface the cytoskeleton and membrane will deform. The deformation of the cell and punctuate binding of cell adhesion proteins can give rise to membrane tethers several micrometers in length. Such tether formation has been observed in model systems and whole cells [36, 37]. Increasing contact times and forces have also been found to result in an increase in the required pulling distance to separate a cell from a surface, due to the potential for a larger number of bonds to form over time, clustering of proteins into higher order structures over time, or as a result of a larger contact area with a higher contact force. As such, an extended 100 µm pulling range is required.

It is technically ambitious to combine the capacity for long-distance and high resolution force measurements in one instrument. Piezo driven movement is associated with background noise. Hence, for high resolution imaging the maximum range of the z-piezo has been deliberately limited, usually to a range of less than 15 µm in AFMs that are suitable for most biomedical applications. However, a piezo with a longer range is a prerequisite for cell-cell unbinding measurements. The CellHesion™ module (JPK Instruments, Berlin, Germany) is a technical solution for these problems. The module contains a sample stage that is fitted with piezo elements that have a 100 µm range for moving the sample in the z-direction. It extends the pulling range for long distance force-spectroscopy without diminishing imaging capabilities of the instrument. As the instrument is installed on an inverted light microscope, the

objective can also be fitted with an automated focussing device in order to maintain the focus plane of the cantilever bound cell when it is moved. In order to precisely control the contact conditions - the applied force, contact time and pulling speed - the piezo elements are controlled by a closed-loop system. Closed loop systems integrate feedback signals in real time to compensate for the hysteresis inherent in piezo movement, allowing more accurate positioning.

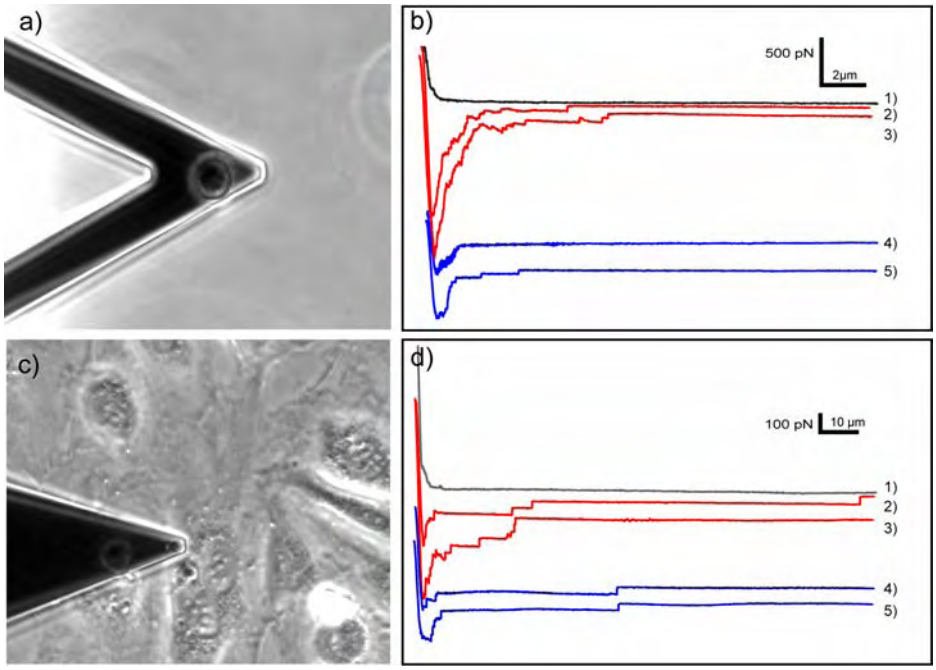

Fig. 6: Force spectroscopy of cantilever bound cells. a) Unbinding of a single melanoma (WM115) cell from a fibronectin coated surface. Single cells were attached to a ConA cantilever and used to probe the surface. The approach and retract speeds were set to 10 µm/sec, cell-surface contact was maintained for 20 sec, and the pulling distance was set to 20 µm. A representative approach curve is presented in grey (c and d, 1). Red curves (c, 2 and 3) correspond to unbinding before blocking with RGD peptide and the blue curves (c, 4 and 5) were acquired after incubation of cells for 30 min in 250 µM of RGD peptide, which competes with FN to bind to the active site of integrins. In the retract curves, before blocking, there were a number of small unbinding events (44 ± 8 pN). Many of these were preceded by a force plateau (corresponding to tether formation). The maximal unbinding force was reduced after incubation with RGD peptide and the number of unbinding events reduced. **b)** Unbinding of WM115 melanoma cells from an endothelial cell layer (human umbilical vein cells). Typical force curves are displayed for different contact times. The approach speed was set to a speed of 10 µm/sec (d, 1). After reaching a preset force, the contact was maintained for the 5 (d, 2&4) or 20 (d, 3&5) seconds (at a constant position on the z-piezo) and then the cells were separated at 10 µm/sec. Small adhesion events were recorded at long cell-surface distances when calcium was present in the medium (d, 2&3). Some were preceded by long force plateaus (several micrometers) that are likely to be the signature of membrane tethers. When calcium was removed by the addition of EGTA (d, 4&5), the maximal unbinding force was reduced, the number of small de-adhesion events decreased, but their magnitude stayed the same (not shown), and the maximal pulling length needed for separating the cells was notably shorter.

This "nano-forklift" approach has been used to study various systems including aggregation of *Dictyostelium discoideum* cells, the binding of leukocytes to endothelial cell layers, the role of adhesion during gastrulation in zebrafish and the early stages of integrin mediated binding of cells to collagen I substrates [31, 38-41]. The technique not only has potential for the quantification of forces involved in cell adhesion, but also to investigate adhesion as an effector mechanism [30, 39, 40]. As such, it is a powerful tool to analyze cell adhesion in cancer development and metastasis. As an example, melanoma cells (WM115) from a primary tumor site were attached to a conconavalin A-coated cantilever and used to probe a fibronectin coated surface (Fig. 6a) and a monolayer of HUVEC cells (Fig. 6b). After an initial set of force-distance curves was obtained on the target surface (2 and 3, Fig. 6c, d) the activity of specific surface adhesion molecules was blocked before collecting a second set of force-distance curves to determine the influence of the given surface protein on adhesion (4 and 5, Fig. 6c, d). Blocking integrin binding to integrins by RGD peptide resulted in a reduction in both the maximal unbinding force, as well as the number of discrete interactions between the probe cell and the surface. A similar effect on melanoma cell- HUVEC cell binding was noted when cadherin activity was impaired by removing calcium ions from the media by adding EGTA. This technique can be used to characterize the function and regulation of specific CAMs [38-41].

4. Force Mapping and AFM optical microscopy Integration

4.1 Rationale

The extracellular matrix is not an inert, passive framework. Instead, it displays an astonishing degree of structural and functional alteration upon remodelling. Dynamic interactions at the cell-ECM interface and the nanomechanics of tumor cell invasion can be investigated by the simultaneous biophysical probing of cellular subdomains and pericellular ECM by AFM. The combination of AFM with conventional fluorescence microscopy can complement this information i.e. to clarify the spatial and temporal relationship of intra- and extracellular events.

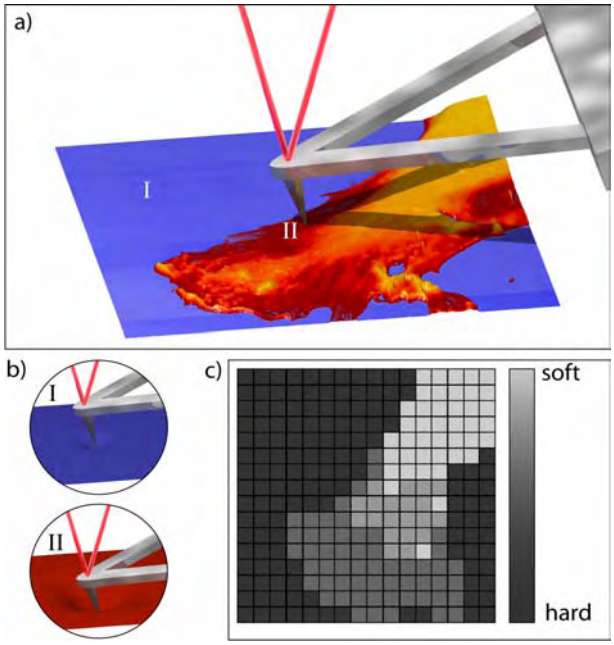

Fig. 7: Elasticity Mapping. a) The AFM tip can be used for direct probing of small sample areas. **b)** If the AFM-tip is moved directly towards a stiff surface (i.e. the glass of a coverslip), deflection of the cantilever is proportional to the piezo driven vertical displacement **(I)**. In soft samples, such as a cell's leading edge, indentation of the surface results in a discrepancy of deflection signal and piezo travel **(II)**. **c)** Probing surface properties in a raster-like fashion will result in a "force-map". Modern AFMs can automatically generate such a map by probing up to 256 x 256 spots in a selected region. The resulting force-map displays the distribution of the mechanical properties of the scanned area. This information can then be directly correlated with the previously acquired morphometric image.

4.2 Force Mapping

By using the AFM tip as a nanoprobe, biophysical parameters such as the local elasticity of extracellular matrix and the plasma membrane can be quantified and integrated in three dimensional maps. The AFM tip is able to probe an extremely small interaction area (tip radius in the range of 5 to 10 nm) with sensitivity in the pico-Newton range. This corresponds to the order of magnitude of forces that are required to separate i.e. receptors from ligands, unfold proteins or to break a single hydrogen bond [32, 42, 43].

Furthermore, an automatically recorded 2D array of force plots can be integrated in one 3D map, where the third dimension encodes sample stiffness (Fig. 8l). Although the basis of force mapping is given and has already been used in a variety of applications, this method is still challenging and specific protocols have to be developed for each application.

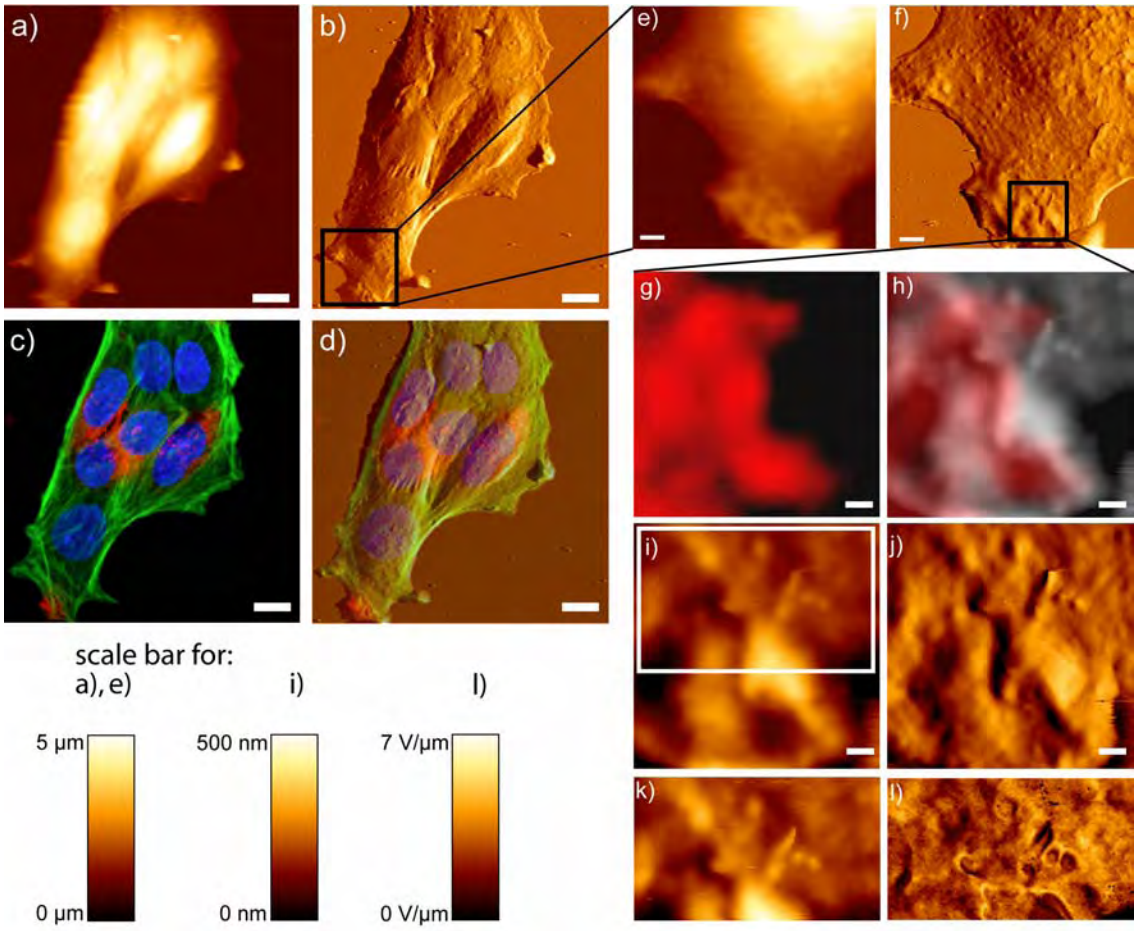

Fig. 8: Combined AFM and confocal imaging of mouse embryonic fibroblasts. a-d) A contact mode AFM image and a calibrated, cofocal microscopic image of the same sample were overlaid to combine the AFM's 3D morphometric data with fluorescence information. **a)** heigt topography **b)** cantilever deflection **c)** laser scanning cofocal image, and **d)** overlay of AFM height and confocal image. Higher resolution images were acquired by zooming into the marked regions. **e and i)** height and **f and j)** cantilever deflection images. **g)** confocal and **h)** overlay of confocal and AFM image. A high resolution force map was generated with an applied force of 200 pN. **k)** Topography represents the height of the piezo at which the setpoint was reached (200 pN) and **l)** the slope of the indentation curve represents a basic measure for stiffness. (scale bars: a-d = 10µm, e-f = 2 µm and g-j = 500 nm; staining: nucleus (DAPI), actin (FITC phalloidin), clathrin (rabbit anti clathrin heavy chain/ TRITC goat anti rabbit)).

4.3 Combination of AFM and optical Microscopy

Several novel AFMs have been designed for the integration of optical microscopy [44-46]. These can be installed on an inverted light microscope, without disrupting the transmission light path. With transparent sample supports, such as coverglass, AFM imaging can be combined with optical techniques such as phase contrast, DIC, epifluorescence, laser scanning confocal microscopy (LSCM) and total internal reflection fluorescence (TIRF). This combination of AFM with light microscopy is crucial for the effective *in vitro* investigation of cells and biological systems. However for true optical integration with AFM, more is required than just the colocalization of the two microscopes. Optical microscopy is based on the use of lenses and any aberrations in such lenses will lead to distortions in the final image. As such, in most cases the AFM image and the light microscopy image do not accurately overlay, with shear or stretch in the optical image as a common problem. If the AFM image is generated using very precise, linearized piezo-electric elements (correct to 0.3 nm in x- and y-direction) this means that the AFM image can be treated as "real-space". The cantilever can be manoeuvred to defined points, which can be utilized to calibrate the optical image. In brief, for one technical solution named "Direct Overlay" (JPK Instruments, Berlin, Germany) the cantilever is moved to a set of 25 points. An optical image is acquired at each point and the tip is automatically located within the optical image. A transform function is calculated using th two sets of reference points and the calibrated optical image can then be imported into the AFM software platform (Fig. 8). This allows the accurate, online comparison of AFM and light microscopic information.

5. Perspectives

Basic research has to close significant gaps in our understanding of the remodelling of the cellular microenvironment. The disappointing results of several clinical trials with protease inhibitors stress the importance to further our understanding of substantial aspects of tumor cell biology. The limitations of conventional state of the art methods offer unique opportunities for innovative, nanotechnology based approaches that enable both - high resolution imaging and direct probing of biophysical parameters. Atomic Force Microscopy is the prototype of a technology that meets these requirements and accordingly its applications in biomedical research are rapidly evolving.

Acknowledgements: We thank Professor Daniel Mueller and his laboratory, particlularly Pierre_Henry Puech (University of Technology Dresden, Germany) for their generous support. Imaging was performed with a NanoWizard II (JPK Instruments, Berlin, Germany) and confocal imaging with a C1 (Nikon). Data analysis and image generation were performed with the Scanning Probe Image Processor, SPIP (Image Metrology, Lyngby, Denmark) and JPK software. The research presented here has been supported by the Deutsche Forschungsgmeinschaft (DFG grants LU854/2-1, LU854/2-2 and LU854/3-1). CellHesion™ is a registered trademark of JPK Instruments.

References

[1] Hanahan, D. & Weinberg, R. A. (2000) *Cell* 100, 57-70.
[2] Sporn, M. B. (1996) *Lancet* 347, 1377-1381.
[3] Ludwig, T. (2006) in *Nanomaterials for Cancer Diagnosis*, ed. Kumar, C.; John Wiley & Sons, Ltd., pp. 377-412.
[4] Liotta, L. A. & Kohn, E. C. (2003) in *Cancer Medicine* (B.C. Decker.
[5] Liotta, L. A. & Stetler-Stevenson, W. G. (1991) *Cancer Res.* 51, 5054s-5059s.
[6] Bogenrieder, T. & Herlyn, M. (2003) *Oncogene* 22, 6524-6536.
[7] Ludwig, T. (2005) *Bioessays* 27, 1181-1191.
[8] Liotta, L. A., Tryggvason, K., Garbisa, S., Hart, I., Foltz, C. M., & Shafie, S. (1980) *Nature* 284, 67-68.
[9] Ludwig, T., Ossig, R., Graessel, S., Wilhelmi, M., Oberleithner, H., & Schneider, S. W. (2002) *Am. J. Physiol Renal Physiol* 283, F319-F327.

[10] Sternlicht, M. D. & Werb, Z. (2001) *Annu. Rev. Cell Dev. Biol.* 17, 463-516.
[11] Egeblad, M. & Werb, Z. (2002) *Nature Rev. Cancer* 2, 161-174.
[12] Stamenkovic, I. (2003) *J Pathol.* 200, 448-464.
[13] Yu, W. H., Woessner, J. F., Jr., McNeish, J. D., & Stamenkovic, I. (2002) *Genes Dev.* 16, 307-323.
[14] Powell, W. C., Fingleton, B., Wilson, C. L., Boothby, M., & Matrisian, L. M. (1999) *Curr. Biol.* 9, 1441-1447.
[15] Mitsiades, N., Yu, W. H., Poulaki, V., Tsokos, M., & Stamenkovic, I. (2001) *Cancer Res.* 61, 577-581.
[16] Schlondorff, J. & Blobel, C. P. (1999) *J Cell Sci.* 112 (Pt 21), 3603-3617.
[17] Page-McCaw, A., Ewald, A. J., & Werb, Z. (2007) *Nat. Rev. Mol. Cell Biol.* 8, 221-233.
[18] Hiraoka, N., Allen, E., Apel, I. J., Gyetko, M. R., & Weiss, S. J. (1998) *Cell* 95, 365-377.
[19] Genis, L., Galvez, B. G., Gonzalo, P., & Arroyo, A. G. (2006) *Cancer Metastasis Rev.* 25, 77-86.
[20] Overall, C. M. & Blobel, C. P. (2007) *Nat. Rev. Mol. Cell Biol.* 8, 245-257.
[21] Lopez-Otin, C. & Overall, C. M. (2002) *Nat. Rev. Mol. Cell Biol.* 3, 509-519.
[22] Baro, A. M., Miranda, R., Alaman, J., Garcia, N., Binnig, G., Rohrer, H., Gerber, C., & Carrascosa, J. L. (1985) *Nature* 315, 253-254.
[23] Kusick, S., Bertram, H., Oberleithner, H., & Ludwig, T. (2005) *J Cell Physiol* 204, 767-774.
[24] Schneider, S. W., Larmer, J., Henderson, R. M., & Oberleithner, H. (1998) *Pflugers Arch.* 435, 362-367.
[25] Koshikawa, N., Giannelli, G., Cirulli, V., Miyazaki, K., & Quaranta, V. (2000) *J Cell Biol* 148, 615-624.
[26] Belien, A. T., Paganetti, P. A., & Schwab, M. E. (1999) *J Cell Biol.* 144, 373-384.
[27] Nabeshima, K., Inoue, T., Shimao, Y., Okada, Y., Itoh, Y., Seiki, M., & Koono, M. (2000) *Cancer Res.* 60, 3364-3369.
[28] Sanceau, J., Truchet, S., & Bauvois, B. (2003) *J Biol. Chem.* 278, 36537-36546.
[29] Stolz, M., Raiteri, R., Daniels, A. U., VanLandingham, M. R., Baschong, W., & Aebi, U. (2004) *Biophys. J* 86, 3269-3283.
[30] Puech, P. H., Taubenberger, A., Ulrich, F., Krieg, M., Muller, D. J., & Heisenberg, C. P. (2005) *J. Cell Sci.* 118, 4199-4206.
[31] Benoit, M., Gabriel, D., Gerisch, G., & Gaub, H. E. (2000) *Nat. Cell Biol.* 2, 313-317.
[32] Rief, M., Gautel, M., Oesterhelt, F., Fernandez, J. M., & Gaub, H. E. (1997) *Science* 276, 1109-1112.
[33] Hinterdorfer, P., Baumgartner, W., Gruber, H. J., Schilcher, K., & Schindler, H. (1996) *Proc. Natl. Acad. Sci. U. S. A* 93, 3477-3481.
[34] Oesterhelt, F., Oesterhelt, D., Pfeiffer, M., Engel, A., Gaub, H. E., & Muller, D. J. (2000) *Science.* 288, 143-146.
[35] Oberleithner, H., Riethmuller, C., Ludwig, T., Shahin, V., Stock, C., Schwab, A., Hausberg, M., Kusche, K., & Schillers, H. (2006) *J. Cell Sci.* 119, 1926-1932.
[36] Benoit, M. & Gaub, H. E. (2002) *Cells Tissues. Organs.* 172, 174-189.
[37] Chu, Y. S., Dufour, S., Thiery, J. P., Perez, E., & Pincet, F. (2005) *Phys. Rev. Lett.* 94, 028102.
[38] Wojcikiewicz, E. P., Zhang, X., Chen, A., & Moy, V. T. (2003) *J. Cell Sci.* 116, 2531-2539.
[39] Wojcikiewicz, E. P., Zhang, X., & Moy, V. T. (2004) *Biol. Proced. Online.* 6:1-9.
[40] Ulrich, F., Krieg, M., Schotz, E. M., Link, V., Castanon, I., Schnabel, V., Taubenberger, A., Mueller, D., Puech, P. H., & Heisenberg, C. P. (2005) *Dev. Cell.* 9, 555-564.
[41] Taubenberger, A., Cisneros, D. A., Friedrichs, J., Puech, P. H., Muller, D. J., & Franz, C. M. (2007) *Mol. Biol. Cell.* 18, 1634-1644.
[42] Grandbois, M., Beyer, M., Rief, M., Clausen-Schaumann, H., & Gaub, H. E. (1999) *Science* 283, 1727-1730.
[42] Engel, A., Gaub, H. E., & Muller, D. J. (1999) *Curr. Biol.* 9, R133-R136.
[44] Franz, C. M. & Muller, D. J. (2005) *J. Cell Sci.* 118, 5315-5323.
[45] Poole, K. & Muller, D. (2005) *Br. J. Cancer.* 92, 1499-1505.
[46] Poole, K., Khairy, K., Friedrichs, J., Franz, C., Cisneros, D. A., Howard, J., & Mueller, D. (2005) *J. Mol. Biol.* 349, 380-386.